THREE PHASE SINE WAVE VOLTAGE SOURCE INVERTER
USING THE SOFT SWITCHED RESONANT POLES

Jung G. Cho, Dong Y. Hu and *Gyu H. Cho*

Dept. of Electrical Engineering, Korea Advanced Institute of Science and Technology
P.O.Box 150 Chongryang, Seoul 130-650, Korea

ABSTRACT

A zero voltage switching based three phase voltage source inverter is presented. The soft switched resonant pole which is obtained by generalizing the conventional pseudo-resonant pole, is presented and suitable control and modeling methods are also described. The three phase resonant pole inverter is easily obtained by connecting three resonant poles to voltage source in parallel and it can be operated on higher power level than the conventional resonant dc-link inverters with the same ratings of devices since the device stresses are lower. Further, it shows high quality spectral performance close to sinusoidal waveform, due to the filtering action of LC elements. Analysis and simulation results are shown to verify the operating principle of the proposed three phase resonant pole inverter.

I. INTRODUCTION

In recent years, high frequency link ac-ac converters have been hot issues in power-conversion systems because of their well known merits such as high power density, high efficiency and high performance.

The high frequency resonant ac-link converters are well established[1-2] and they are relatively easy to control by pulse density modulation. So far, these resonant ac-link converters, however, are known as not cost effective since all of the switches must be bidirectional. The resonant dc-link converters can be obtained by adding dc-offset to ac-link circuit.[3-4] These converters have simple unidirectional switch structures like as those of conventional hard switched bridge converters. However, the device stresses are highly increased due to the dc offset of link circuit, which also gives more serious effect to the transistorized parallel resonant dc-link inverter[3]. To reduce link voltage stress of the resonant dc-link inverter, several methods have been proposed.[5-7] Two clamping methods, passive voltage clamping(2.5Vs approximately) and active voltage clamping(1.3-1.8Vs), have been proposed.[5] The
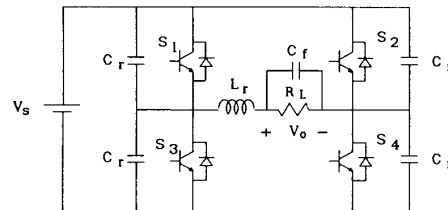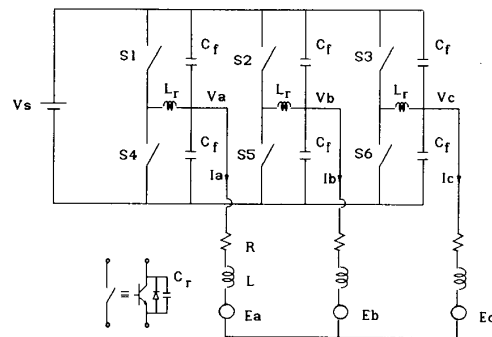

Fig. 1 Circiut schematic of single phase RPI

Fig. 2 Proposed three phase RPI with induction motor load

link voltage could be reduced considerablely by using the active clamping method, however, the active clamping shows some difficulty in operation during transition from powering mode to regenerating mode. A programmable initial current control method has been proposed.[7] It limits the link voltage to 2Vs and assures zero voltage switchings under all conditions of inverter operation. However, power circuit is complicated due to the initial current control circuit and link voltage is still high as compared to the conventional PWM voltage source inverter.

Another approach for high power density inverter with low device voltage stress is zero voltage switching based resonant pole inverter(RPI).[5,6] The topology of single phase RPI which is obtained by modifying the conventional pseudo

48

resonant pole[8] is shown in Fig. 1. The RPI is fed from the dc voltage source and the parallel capacitors with the switches resonate only during the short switching intervals to make zero voltage switching condition. The device voltage stress is very low(limited to V_s) and output voltage is easily controlled with high spectral performance. So, the RPI can be operated to higher power levels than resonant dc-link inverter with the same ratings of the devices. However, the single phase RPI shown in Fig. 1 is not easy to be extended to three phase inverter with modified pseudo resonant pole.

In this paper, the three phase RPI using the soft switched resonant poles is presented. The soft switched resonant pole which is obtained by generalizing the conventional pseudo-resonant pole[8], is presented and suitable control and modeling methods are also described. The three phase RPI can easily be obtained by connecting the three resonant poles to voltage source in parallel as shown in Fig. 2 and it is easy to control since each pole can be controlled independently. Further, the three phase RPI has high spectral performance because of filtering action of LC elements. Detailed analysis and computer simulation results are presented to verify the operating principle.
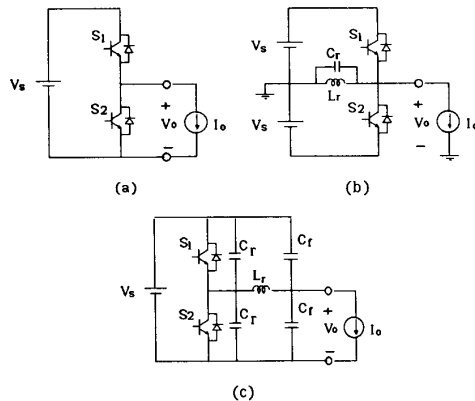

Fig. 3 (a) Conventional hard switched pole
(b) Pseudo-resonant pole
(c) proposed resonant pole

II. THE SOFT SWITCHED RESONANT POLE

A. Topology of the Resonant Pole

The proposed resonant pole and the other two poles are shown in Fig. 3, for comparison. As shown in Fig. 3(a), the conventional hard switched pole is simple and well known. The switching losses of the two switches, however, are considerably high because of hard switching. To reduce the switching loss, zero voltage switching based pseudo resonant pole is proposed by D. M. Divan as shown in Fig. 3(b).[8] The operation of the pseudo resonant pole is also simple and well know. The inductor current is linearly increased and decreased with zero average value except resonant region and its peak to peak

current must be greater than $2I_o$ for assuring zero voltage switching. Since the peak to peak inductor current which does not contribute to power transfer is increased according to load current, the large amount of conduction loss occurs. To apply the pseudo resonant pole to inverter, it is modified so that the inductor current plays major role in the power transfer process. The single phase RPI is obtained by using the modified pseudo resonant pole as shown in Fig. 1.[6] However, it is not easy to obtain the three phase RPI by using the modified pseudo resonant pole.

To apply the modified pseudo resonant pole to the three phase inverter, it is separated independently like the hard switched pole using the capacitor filter C_f(voltage source) as shown in Fig. 3(c). The resonant capacitor C_r and filter capacitor C_f are arranged symmetrically. A similar scheme has been presented for dc/dc converter(inverter)[9] and its operation is also very similar. By connecting three soft switched resonant poles, three phase RPI is obtained as previously shown in Fig. 2.
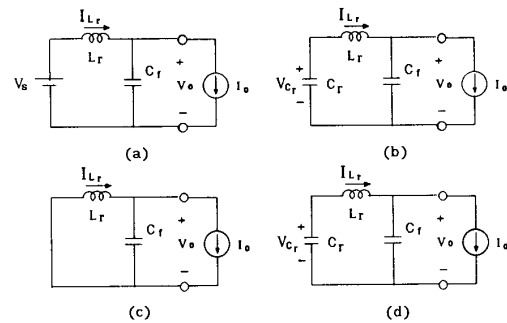

Fig. 4 Equivalent circuits for each mode
(a) mode 1 (S1:on, S2:off)   (b) mode 2 (S1:off, S2:off)
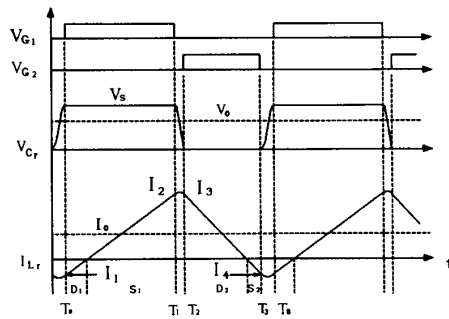(c) mode 3 (S1:off, S2:on)   (d) mode 4 (S1:off, S2:off)

Fig. 5 Switching waveforms of the resonant pole

B. Steady State Analysis

The steady state operations are analyzed by assuming the filter capacitor C_f as constant voltage source over a switching cycle. One switching cycle can be divided into four modes and the associated equivalent circuits are shown in Fig. 4. Suppose that the two switches are all off and the initial

49

resonant capacitor voltage and resonant inductor current are V_s and I_1, respectively. A time T_0, the switching cycle starts by turning on S_1 with zero voltage condition.

(i) Mode 1 (T_0, T_1); S_1: on, S_2: off

As shown in Fig. 4(a), the capacitor voltage V_{C_r} is replaced by source voltage V_s. Then, the inductor current I_{L_r} is increased linearly with given initial current I_1 as

$$I_{L_r}(t) = \frac{V_s - V_o}{L_r} \cdot t + I_1. \tag{1}$$

At time T_1, the inductor current reaches its positive reference value I_2 and we obtain

$$I_2 = \frac{V_s - V_o}{L_r} \cdot T_1 + I_1. \tag{2}$$

(ii) Mode 2 (T_1, T_2): S_1: off, S_2: off

At time T_1, the switch S_1 is turned off with zero voltage condition and $L_r C_r$ begins to resonate with the initial conditions, I_2 and V_s, respectively. In this case, I_{L_r} and V_{C_r} become

$$I_{L_r}(t) = I_2 \cdot cos(\omega_r t) + \frac{V_s - V_o}{Z_r} \cdot sin(\omega_r t) \tag{3}$$

$$V_{C_r}(t) = (V_s - V_o) \cdot cos(\omega_r t) - I_2 Z_r \cdot sin(\omega_r t) + V_o \tag{4}$$

where, $\omega_r = (L_r C_r)^{-1/2}$ and $Z_r = (L_r / C_r)^{1/2}$. The capacitor voltage V_{C_r} resonates and reaches zero at time T_2 when I_{L_r} reaches I_3 as

$$I_3 = [I_2^2 + \frac{V_s}{Z_r^2}(V_s - 2V_o)]^{1/2}. \tag{5}$$

(iii) Mode 3 (T_2, T_3); S_1: off, S_2: on

In this mode, the capacitor voltage V_{C_r} is kept zero and the inductor current I_{L_r} begins to decrease linearly from its initial value I_3 to its negative reference I_4:

$$I_{L_r}(t) = -\frac{V_o}{L_r} \cdot t + I_3. \tag{6}$$

At time T_3, the inductor current reaches I_4 which is given by

$$I_4 = -\frac{V_o}{L_r} \cdot (T_3 - T_2) + I_3. \tag{7}$$

(iv) Mode 4 (T_3, T_s); S_1: off, S_2: off

At time T_3, the switch S_2 is turned off with zero voltage condition and $L_r C_r$ begins to resonates with initial conditions, I_4 and 0, respectively:

$$I_{L_r}(t) = I_4 \cdot cos(\omega_r t) - \frac{V_o}{Z_r} \cdot sin(\omega_r t) \tag{8}$$

$$V_{C_r}(t) = -V_o \cdot cos(\omega_r t) - I_4 Z_r \cdot sin(\omega_r t) + V_o. \tag{9}$$

When $V_{C_r}(t) = V_s$, the switch S_1 is turned on with zero voltage condition. If the inductor current reaches the initial value of mode 1, then a switching cycle is completed and we obtain

$$I_1 = [I_4^2 - \frac{V_s}{Z_r^2}(V_s - 2V_o)]^{1/2}. \tag{10}$$

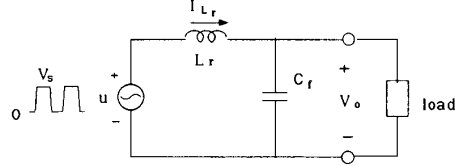The overall switching waveforms are shown in Fig. 5.
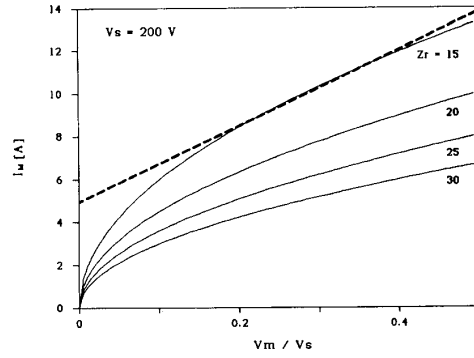

Fig. 6 Equivalent circuit of resonant pole

Fig. 7 Minimum initial inductor for normalized output voltage amplitude

C. Hysteresis Current Control

The soft switched resonant pole circuit of Fig. 3(c) can be redrawn equivalently as shown in Fig. 6. To assure zero voltage switching, the initial inductor current must be greater than a certain minimum value I_M. If the amplitude of output voltage is denoted to $V_m (= |V_o - V_s/2|)$, the minimum initial current I_M can be given as follows

$$I_M = \frac{[2V_s V_m]^{1/2}}{Z_r} \tag{11}$$

and the relation of I_M and the normalized output voltage amplitude V_m / V_s with parameter Z_r is plotted in Fig. 7. To reduced the rms current stress, the I_M must be reduced as small as posible. However, the characteristics of I_M curve is highly nonlinear as shown in Fig. 7. The I_M curve can be fitted roughly by straight line as dotted line in Fig. 7 so that it can be easily implemented. The softed switched resonant pole can be controlled easily by the hysteresis current control method and the closed loop control block diagram with local

hysteresis current control loop is shown in Fig. 8. Two methods are available for hysteresis current control. They are fixed hysteresis band method and variable hysteresis band method as shown in Fig. 9(a) and (b), respectively. In the fixed hysteresis band method, the hysteresis band ΔI is fixed, however, it must be wide enough to be controlled over full current range as follows:

$$\Delta I = 2(I_{\lim} + I_M). \tag{12}$$

The switching frequency is also fixed except the transient because of fixed hysteresis band. We can see that this method is inefficient because large amount of conduction loss occurs. The variable hysteresis band method is similar to the control method of single phase RPI.[6] The initial inductor current can be kept minimum value I_M by varying hysteresis band. The hysteresis band ΔI is varied according to the reference current I_R as follows:

$$\Delta I = 2(I_R + I_M). \tag{13}$$

The switching frequency is also varied as shown in Fig. 10 since it is inversely proportional to the hysteresis band. The upper limit of switching frequency is determined by I_M and resonant period(duration of mode 2,4 in Fig. 5), on the other hand, the lower limit is determined by the maximum reference current $I_{\lim}$.
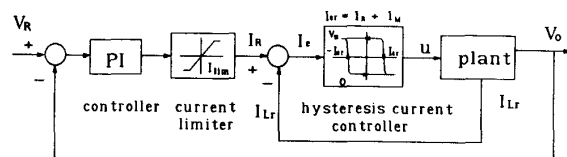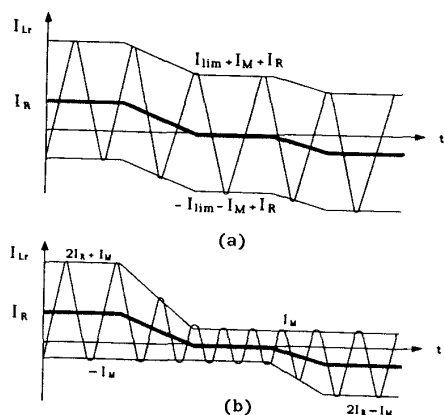

Fig. 8 Closed loop block diagram

Fig. 9 Illustrative inductor current waveform for hysteresis current control with
(a) fixed hysteresis band
(b) variable hysteresis band

The global loop for the output voltage control can be achieved by the conventional PI-controller. Since the open loop system is type zero, the integral action must be included in the controller to eliminate steady state error. The simulation of the resonant pole with ideal current source load is shown in Fig. 11. We can see that the output voltage follows its reference very well with low ripple.

D. Modelling and Controller Design

To design controller with the conventional design technique, plant must be modeled as a time invariant system. The resonant pole which is controlled by hysteresis current control method, can be modeled by assuming the output voltage varies much slowly compared to the variation of the inductor current as shown in Fig. 12. Fig. 13 shows the overall control block diagram with modeled time invarient system. Thus, we can design PI-controller by using the conventional design techniques.
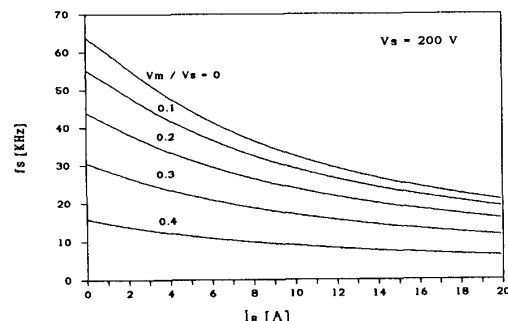

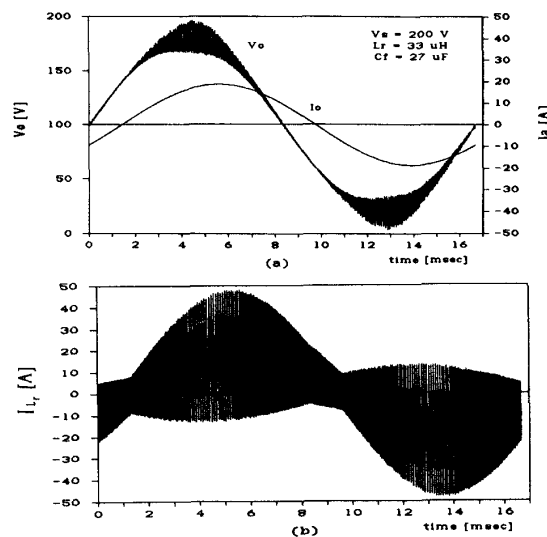Fig. 10 Varitions of the switching frequency for reference current.

Fig. 11 Simulation of the resonant pole with ideal current source
(a) pole output voltage and load current
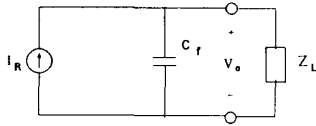(b) resonant inductor current

54

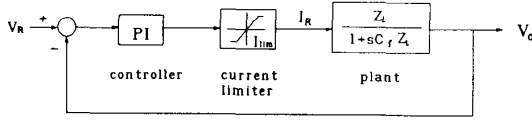Fig. 12 Modeling of the hysteresis current controlled pole

Fig. 13 Simplified block diagram for controller design

III. CONSTRUCTION OF THREE PHASE RPI

The three phase resonant pole inverter can be easily constructed by connecting the three proposed resonant poles to the voltage source in parallel as shown in Fig. 2. The topological configuration is very similar to that of the conventional PWM voltage source inverter except LC resonant and filter elements for zero voltage switching. So, it can also be thought as the conventional PWM voltage source inverter with LC filter and the size of LC filter can be designed small enough to ignore the dynamics of RPI itself comparing to load dynamics. Therefore, the RPI has high spectral performance without deteriorating of overall dynamics.

The control of the phase voltages of RPI is also very simple because each pole can be controlled independently with any voltage and any frequency. To obtain the phase voltage whose amplitude and frequency are V_m and ω, respectively, the voltage reference of each pole can be given as follows.

$$V_{Ra} = V_m \cdot sin(\omega t) + \frac{V_s}{2} \tag{14}$$

$$V_{Rb} = V_m \cdot sin(\omega t - \frac{2\pi}{3}) + \frac{V_s}{2} \tag{15}$$

$$V_{Rc} = V_m \cdot sin(\omega t + \frac{2\pi}{3}) + \frac{V_s}{2} \tag{16}$$

Then, the line-to-line voltage becomes

$$V_{ab} = \sqrt{3} V_m \cdot sin(\omega t - \frac{\pi}{6}). \tag{17}$$

IV. SIMULATION RESULTS

The three phase RPI is simulated with induction motor load to prove its operation. The parameters of RPI and the induction motor which is modeled simply by R-L load with back emf, are given as follows:

o inverter parameters :

$$V_s = 200[V], \ C_f = 27[uF], \ L_r = 33[uH], \ C_r = 0.154[uF].$$

o induction motor parameters :

$$R = 2[\Omega], \ L_s = 1[mH], \ E_m = 50[V], \ \phi = 10 \ deg.$$

Fig. 14 shows the simulation results of PRI in the steady state. The waveforms appear to be very satisfactory. The output voltages is obtained with high spectral performance, near sine wave, as shown in Fig. 14(a). Accordingly, the load current has almost zero ripple.
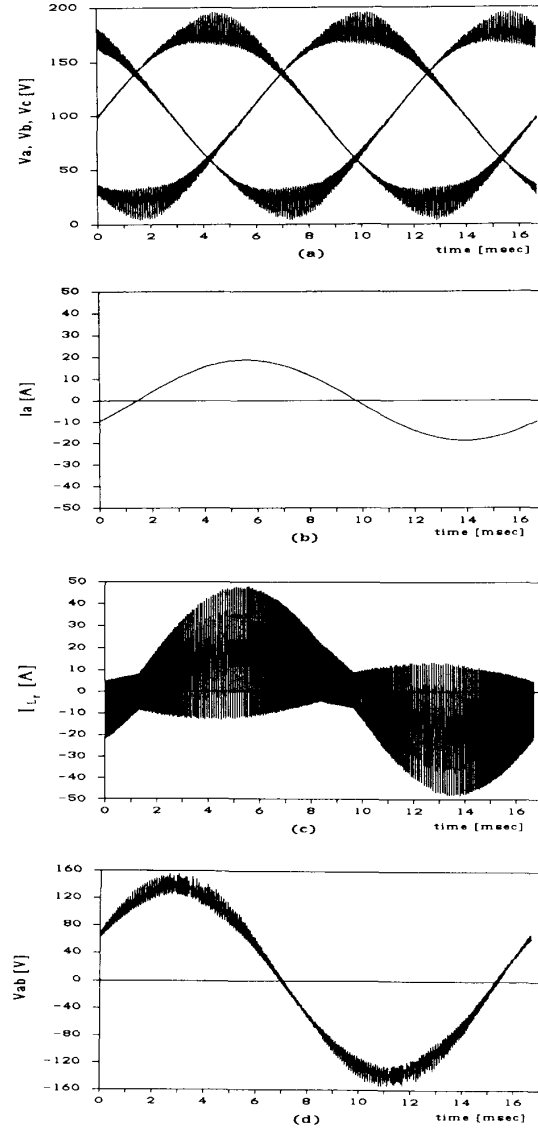

Fig. 14 Simulation of three phase RPI with induction motor load
(a) phase voltage, (b) phase current
(c) inductor current, (d) line-to-line voltage

52

V. CONCLUSION

In this paper, a three phase sine wave voltage source inverter using the soft switched resonant pole is presented and suitable control and modeling methods are also described. The operation of the proposed resonant pole and the three phase RPI is verified through the computer simulation. It is shown that the proposed three phase RPI can be easily obtained by connecting three resonant poles and it is easy to control and analyze. The topological configuration is very similar to that of the conventional PWM voltage source inverter except LC resonant and filter elements. Accordingly, in the sense of global operation, it can be thought as conventional PWM inverter with small size LC filter. Therefore, the proposed three phase RPI features high power density, high efficiency and high spectral performance having an advantage over the conventional PWM inverter such as low device voltage and rms current stresses. So, it can be thought to be useful for ac motor driver with higher power level than the conventional resonant dc-link inverter.

REFERENCES

[1] S. K. Sul and T. A. Lipo, "Design and performance of a high frequency link induction motor drive operating at unity power factor", IEEE IAS Rec., pp. 308-313, 1988.

[2] J. B. Klaassens and E. J. F. M. Smits, "Series-resonant ac-power interface with an optimal power factor and enhanced conversion ratio", IEEE Trans. on Power Electronics, vol. 3, No. 3, pp. 335-343, July 1988.

[3] Y. Murai and T. A. Lipo, "High frequency series resonant dc link power conversion", IEEE IAS Rec., pp. 308-313, 1988.

[4] D. M. Divan, "The resonant dc link converter - A new concept in static power conversion", IEEE IAS Rec., pp. 648-656, 1986.

[5] D. M. Divan and G. Skibinski, "Zero switching Loss inverters for high power applications", IEEE IAS Rec., pp. 627-634, 1987.

[6] D. M. Divan and G. Venkataramanan R. W. De Doncker, "Design methodologies for soft switched inverters", IEEE IAS Rec., pp. 754-766, 1988.

[7] J. S. Lai and B. K. Bose, "An improved resonant dc link inverter for induction motor drives", IEEE IAS Rec., pp. 754-766, 1988.

[8] O. D. Patterson and D. M. Divan, "Pseudo-resonant full bridge dc-dc converter", IEEE PESC Rec., pp.424-430, 1987.

[9] D. M. Divan, "Diode as pseudo-active elements in high-frequency dc/dc converters", IEEE Tr. PE, Vol.4, No.1, Jan. 1989.